OFFICE OF NAVAL RESEARCH

Grant N00014-90-J-1193

TECHNICAL REPORT No. 73

Kinetics of Intersubband Optical Excitation and Photoinduced Electron Transfer in an Asymmetric Double Quantum Well

by

Mark I. Stockman, Leonid S. Muratov, Lakshmi N. Pandey and Thomas F. George

Prepared for publication

in

Physical Review B

Departments of Chemistry and Physics
Washington State University
Pullman, WA 99164-1046

January 1992

8c. ADDRESS (City, State, and ZIP Code)	10. SOURCE OF FUNDING NUMBERS			
Chemistry Program 800 N. Quincy Street Arlington, Virginia 22217	PROGRAM ELEMENT NO.	PROJECT NO.	TASK NO.	WORK UNIT ACCESSION NO.

11. TITLE (Include Security Classification)
Kinetics of Intersubband Optical Excitation and Photoinduced Electron Transfer in an Asymmetric Double Quantum Well

12. PERSONAL AUTHOR(S)
Mark I. Stockman, Leonid S. Muratov, Lakshmi N. Pandey and Thomas F. George

13a. TYPE OF REPORT	13b. TIME COVERED	14. DATE OF REPORT (Year, Month, Day)	15. PAGE COUNT
	FROM _____ TO _____	January, 1992	30

16. SUPPLEMENTARY NOTATION
Prepared for publication in Physical Review B

17. COSATI CODES			18. SUBJECT TERMS (Continue on reverse if necessary and identify by block number)	
FIELD	GROUP	SUB-GROUP	DOUBLE QUANTUM WELL	PHOTOINDUCED
			ASYMMETRIC	INTERSUBBAND EXCITATION
			ELECTRONIC TRANSFER	KINETICS

19. ABSTRACT (Continue on reverse if necessary and identify by block number)

Optical excitation of electrons in an asymmetric double quantum well is theoretically examined. The well is biased to align the excited levels and permit resonant electron tunneling. Emphasis is made on the photoinduced transfer of electrons counter to the bias electric field force. Systems with a weak polarization relaxation (dephasing) are studied using the conventional technique of the Schrödinger equation. A density matrix approach is developed to describe optical excitations in the presence of an arbitrary dephasing. Quantum beats, which follow a short-pulse excitation of the double well, are shown to crucially depend on the dephasing. The excitation profiles obtained for cases of different dephasing reveal the full range of tunneling coupling between the wells from completely coherent to incoherent (stepwise).

20. DISTRIBUTION / AVAILABILITY OF ABSTRACT	21. ABSTRACT SECURITY CLASSIFICATION	
☒ UNCLASSIFIED/UNLIMITED ☒ SAME AS RPT. ☐ DTIC USERS	Unclassified	
22a. NAME OF RESPONSIBLE INDIVIDUAL	22b. TELEPHONE (Include Area Code)	22c. OFFICE SYMBOL
Dr. David L. Nelson	(202) 696-4410	

Physical Review B, in press

KINETICS OF INTERSUBBAND OPTICAL EXCITATION AND PHOTOINDUCED ELECTRON TRANSFER IN AN ASYMMETRIC DOUBLE QUANTUM WELL

Mark I. Stockman, Leonid S. Muratov*, and Lakshmi N. Pandey*
Departments of Physics and Chemistry
Washington State University
Pullman, Washington 99164-2814

Thomas F. George
Departments of Chemistry and Physics
Washington State University
Pullman, Washington 99164-1046

Optical excitation of electrons in an asymmetric double quantum well is theoretically examined. The well is biased to align the excited levels and permit resonant electron tunneling. Emphasis is made on the photoinduced transfer of electrons counter to the bias electric field force. Systems with a weak polarization relaxation (dephasing) are studied using the conventional technique of the Schrödinger equation. A density matrix approach is developed to describe optical excitations in the presence of an arbitrary dephasing. Quantum beats, which follow a short-pulse excitation of the double well, are shown to crucially depend on the dephasing. The excitation profiles obtained for cases of different dephasing reveal the full range of tunneling coupling between the wells from completely coherent to incoherent (stepwise).

PACS: 73.40.Gk, 73.20.Dx, 73.50.Pz, 73.40.Kp

INTRODUCTION

The aim of this paper is to theoretically consider processes of optical excitation and electron transfer in an asymmetric double quantum well, i.e., in a system consisting of two different quantum wells coupled by electron tunneling. We will concentrate on intersubband electronic transitions, which are excited by far ir radiation and consider both optically linear and nonlinear effects. We will focus on the effect of the light-induced transfer of electrons from one well to the other one in the double quantum well. It is important that in biased quantum wells such a transfer can occur against the electric field force and with high quantum yield (up to 0.5).

A quantum well is a semiconductor heterostructure (see, e.g., Ref. 1) whose potential confines electrons to a small region. Such confinement brings about quantum splitting of the electron energy bands into subbands separated by excitation energy on the order of $\hbar^2/m^*a^2$, where m^* is the electron effective mass and a is a confinement size (width of the well). In what follows, we will assume that the conduction band states are populated due to a modulation doping of the barrier regions and/or an incoherent optical excitation from the valence band, and consider purely electronic transitions between subbands of the conduction band [often called QWEST (Quantum Well Electronic (inter)Subband Transitions)]. We will also assume the electron density to be small enough to exclude excitonic and other many-body effects.

Much work has been done on the electronic, optical and kinetic properties of semiconductor double quantum wells (see, e.g., Ref. 1 and references cited therein, and also recently published papers[2-13], which are relevant for the present work). A fundamental phenomenon, which is a subject of the study, is resonant tunneling between the quantum wells. A distinctive feature of this phenomenon is a considerable enhancement of the tunneling probability if the energies of the donor and acceptor levels are close enough. To describe theoretically this phenomenon or interpret experimental results, most of the above cited works rely on the use of the Schrödinger equation. In this approach[1], the wave functions of resonant levels in the wells are mixed due to tunneling, and these states repulse forming a doublet separated by the energy $2|\tau|$, where τ is the tunneling amplitude. The tunneling is described by the delocalization of the electron wave function. Such tunneling is often called coherent, and we will follow this terminology. It is well understood (see, e.g., Refs. 3, 4 and 7) that relaxation destroys coherence, and makes tunneling incoherent (stepwise). When the relaxation rate Γ

becomes on order of the tunneling amplitude τ or greater, the incoherent (stepwise) tunneling takes place between non-mixed states.

To describe a general case of an arbitrary relaxation we will use the density matrix technique, which allows one to fully take into account the relaxation, including the dephasing contribution to the polarization relaxation rate. Such contribution, which is usually neglected, may be important. The Schrödinger equation approach will also be used below to describe coherent tunneling for the sake of comparison.

To explain the essence of the electron transfer effect, let us consider an asymmetric double quantum well with an electric field applied perpendicular to the well plane. The schematic of the confining potential and electron levels (subbands) is shown in Fig. 1a with $|1\rangle$ and $|2\rangle$ as the ground states in the narrow (N) and wide (W) wells, respectively. The excited state in the N well is $|3\rangle$, and in the W well $|4\rangle$. Let us assume that the electric field aligns the excited levels $|3\rangle$ and $|4\rangle$, so that tunneling from one excited level to the other one is resonantly enhanced.

Qualitatively, the electron transfer effect is most pronounced in the coherent tunneling case. We should mention that there exists a convincing evidence of feasibility of at least partially coherent tunneling, based on the observation[9] of coherent oscillations in a double quantum well, which has been suggested earlier[6]. Also, the possibility of partially coherent tunneling is witnessed by the observations of the electron transfer kinetics independent of the barrier width[3], and of the resistance resonance in coupled quantum wells[13]. However, it is not known how strongly the observed effects are changed if relaxation, especially polarization relaxation, is appreciable. Below we shall describe a coherent picture of the electron transfer effect and address a general case in Sec. 3.

In the coherent case, the aligned excited states form a doublet, the upper and lower components of which we denote as $|+\rangle$ and $|-\rangle$. The $|\pm\rangle$-state wave functions are delocalized over both the N and W wells due to resonant tunneling. In contrast, the lower levels are not aligned, and the $|1\rangle$ state is basically localized in the N well and $|2\rangle$ in the W well. Since the subband splitting of the W well is smaller, the overall ground state is $|1\rangle$ in the N well (see Fig. 1b). We assume both the electron density and temperature to be not very high, so that only the $|1\rangle$ state is considerably populated.

Suppose that ir light excites an intersubband transition in the N band, i.e. one of the transitions of the type $|1\rangle \rightarrow |\pm\rangle$ shown in Fig. 1b by a wavy arrow. Since the splitting of

the levels in the N well is assumed to be considerably greater, the radiation does not excite a transition in the W well. The electron excited to either of the $|\pm\rangle$ states is quantum-mechanically delocalized over both the wells. Subsequent relaxation brings about electron transitions to the ground states $|1\rangle$ and $|2\rangle$ shown in Fig. 1b by dashed arrows. The transition rates are proportional to the probabilities for an electron to be localized in the corresponding wells and, for aligned levels, are on the same order of magnitude. Thus, with an appreciable probability, the electron comes to the state $|2\rangle$, which is mainly localized in the W well.

Summarizing, a net result of the photoexcitation of the intersubband transition in the N well is a transfer of the electron from the N well to the W well in the direction of the potential increase (see Fig. 1b), i.e. *against* the direction of of the field force. Indeed, the energy needed for such a transfer is taken from the exciting radiation. Note that if the transition in the wide well is excited, the electron transfer would occur in the direction of the field force.

The closest counterpart of the above described effect is the observation by Sauer, Thonke and Tsang[2] of photoinduced space-charge buildup due to asymmetric electron and hole tunneling in coupled quantum wells. The effect of Ref. 2 is similar to the present effect in regard to electron transfer against the electric-field force but, nevertheless, is essentially different in the following respects. First, there is no relaxation involved in charge buildup in Ref. 2, and, as a result, the electron buildup is *minimum* for the levels aligned, while in our case it is *maximum*. Also, for the aligned excited levels after switching off the optical excitation, the charge, which has been transferred between wells, disappears in a time on the order of the resonant tunneling time, while in our case the charge transferred is stable on this temporal scale. Second, the effect[2] is induced by interband transitions, and, therefore, the portion of the photon energy accumulated in the potential energy of a transferred electron is small, as distinct from the present effect based on intersubband transitions. Third, the charge transfer in Ref. 2 is based upon the difference in the tunneling time of the electrons in the conduction band and holes in the valence band, while no conduction-band holes participate and no such requirement is relevant for the present effect.

The Schrödinger equation description is presented in Sec. 2. The density matrix approach is developed in Sec. 3, including obtaining the basic equations (Sec. 3.1), study of the temporal dynamics (Sec. 3.2), stationary solutions (Sec. 3.3) and numerical examples (Sec. 3.4). The results obtained in the paper are discussed in Sec. 4.

2. COHERENT ELECTRON TRANSFER IN SCHRÖDINGER EQUATION FORMALISM

An electron in a heterostructure is characterized by the quantum number of the state in the well $i = 1, 2, +, -$ and the momentum $\mathbf{p}$ of the movement in the well plain, its energy being $\epsilon_i + \mathbf{p}^2/2m^*$, with ϵ_i as the subband edge energy. For typical times of interwell tunneling, which are normally much less then the electron translation relaxation times, one can consider $\mathbf{p}$ as a conserving quantum number. Also, the photon momentum is much less then a characteristic electron momentum, which allows one to consider $\mathbf{p}$ as conserved by the interaction with light. Taking into account that subbands in the well are *highly parallel*, one concludes that the energy of an intersubband transition $j, \mathbf{p} \to i, \mathbf{p}$, either tunneling or electromagnetic, does not depend on $\mathbf{p}$, and is simply the transition energy for the states in the well, $\epsilon_{ij} \equiv \epsilon_i - \epsilon_j$. These arguments allow one to describe electron states in the well and kinetics of the intersubband transitions separately from the lateral movement, as conventionally done.

The maximum counter-field transfer effect occurs at low temperatures $T \ll 1/m^* a^2$, which we assume. The rate equations describing the populations n_i of the states $|i\rangle$, $i = 1, 2, -, +$ have the form

$$\frac{\partial n_1}{\partial t} = -w_\pm n_1 + (\gamma_{1\pm} + w_\pm) n_\pm + \gamma_{12} n_2 \quad , \quad \frac{\partial n_2}{\partial t} = \gamma_{2\pm} n_\pm - \gamma_{12} n_2 \quad , \qquad \frac{\partial n_\pm}{\partial t} = w_\pm n_1 - (w_\pm + \gamma_\pm) n_\pm \quad . \tag{1}$$

Here $\pm$ means either $+$ or $-$; γ_{ji} are phenomenological rate constants for decay from higher- to lower-lying states, $|i\rangle \to |j\rangle$, $i = +, -, 2$, $j = 2, 1$, and $\gamma_\pm = \gamma_{2\pm} + \gamma_{1\pm}$; w_+ and w_- are well known Einstein coefficients for the transitions $|1\rangle \to |+\rangle$ and $|1\rangle \to |-\rangle$, which can conventionally be expressed in terms of the corresponding dipole matrix elements d_{+1} and d_{-1}, $w_\pm = |\mathbf{E}\mathbf{d}_{\pm 1}|^2 \, \Gamma_{\pm 1} \left[(\Omega - \epsilon_{\pm 1})^2 + \frac{1}{4}\Gamma_{\pm 1}^2 \right]^{-1}$, with $\mathbf{E}$ as the amplitude of the light wave and Ω as the light frequency. To simplify notations, we use the system of units in which $\hbar = 1$.

The probability of electron transfer from the N to W well is equal to the population number n_2. Assuming that the radiation excites one of the transitions $|1\rangle \to |+\rangle$ or $|1\rangle \to |-\rangle$, one finds from the stationary solution of Eq. (1) that

$$n_2 = \gamma_{2\pm} w_\pm \left[\gamma_2 \gamma_\pm + w_\pm (2\gamma_2 + \gamma_{2\pm}) \right]^{-1} \quad , \tag{2}$$

where $\gamma_2 \equiv \gamma_{12}$ is the decay constant of the state $|2\rangle$.

For the limiting case of nonsaturating light intensities, $w_\pm \ll \gamma_2\gamma_\pm(2\gamma_2+\gamma_{2\pm})^{-1}$, assuming both transitions $|1\rangle \to |+\rangle$ and $|1\rangle \to |-\rangle$ to occur, and taking into account that the contributions of these transitions are additive, one obtains from Eq. (2)

$$n_2 = \gamma_2^{-1}\left(w_+\gamma_{2+}/\gamma_+ + w_-\gamma_{2-}/\gamma_-\right) \quad . \tag{3}$$

The corresponding expression for the transfer quantum yield Q has the form

$$Q = \left(w_+\gamma_{2+}/\gamma_+ + w_-\gamma_{2-}/\gamma_-\right)\left(w_+ + w_-\right)^{-1} \quad . \tag{4}$$

As one can see from Eqs. (1)-(4), the electron transfer kinetics is determined by the decay constants γ_{ji} and the matrix elements $\mathbf{d}_{\pm 1}$ which, in turn, depend on the wave function mixing between the individual wells. This mixing is described by the probabilities $P_\pm^{(\mathrm{N})}$ and $P_\pm^{(\mathrm{W})}$ for an electron in the mixed $|\pm\rangle$ state to be in the corresponding N or W well.

To find the decay constants γ_{ij}, we invoke a quantum-mechanical idea that the relaxation causes localization, and an electron localizes in the well in which it has experienced the relaxation. This assumption is valid if the nonresonant tunneling rate is small, which is equivalent to neglect of the overlap of the wave functions in different wells (see also below). The decay rate of the excited electron in the N well is equal to the decay rate γ_3 of the state $|3\rangle$ and, similarly, the decay rate in the W well is γ_4 of the $|4\rangle$ state. To determine $d_{\pm 1}$, we take into account that, with neglect of the overlap, the electromagnetic radiation couples the ground state $|1\rangle$, which is mainly localized in the N well, only to the $|3\rangle$ component of the mixed states. From these arguments we find

$$\gamma_{1\pm} = \gamma_3 P_\pm^{(\mathrm{N})} \quad , \quad \gamma_{2\pm} = \gamma_4 P_\pm^{(\mathrm{W})} \quad , \quad |\mathbf{d}_{\pm 1}|^2 = |\mathbf{d}_{31}|^2 P_\pm^{(\mathrm{N})} \quad . \tag{5}$$

An important characteristic of the electron transfer process is the mean quantum yield $\bar{Q}$ for the wide-band radiation, i.e. for light whose spectral width is much greater than the radiation transition widths. It is defined by the expression [cf. Eq. (4)]

$$\bar{Q} = \gamma_2 \int n_2 \mathrm{d}\Omega \left[\int (w_+ + w_-)\,\mathrm{d}\Omega\right]^{-1} \quad . \tag{6}$$

From this, taking into account Eqs. (3) and (5), one obtains

$$\bar{Q} = \gamma_4 \left[P_+^{(\mathrm{N})}P_+^{(\mathrm{W})}/\gamma_+ + P_-^{(\mathrm{N})}P_-^{(\mathrm{W})}/\gamma_-\right]\left[P_+^{(\mathrm{N})} + P_-^{(\mathrm{N})}\right]^{-1} \quad . \tag{7}$$

To determine the transfer probability (2), we need also to estimate the interwell transition constant $\gamma_2 \equiv \gamma_{12}$. Note that γ_2 is proportional to the probability $P_2^{(N)}$ for an electron in the state $|2\rangle$, which is mainly localized in the W well, to appear in the N well and experience a relaxation there. Assuming the relaxation of all states in the N well to occur with the same rate, determined, e.g. by collisions, one can estimate $\gamma_2 \approx \gamma_3 P_2^{(N)}$, and obtain from Eq. (2) the saturated transfer probability

$$n_2^{(s)} = \left(1 + 2\gamma_3 P_2^{(N)}/\gamma_4 P_\pm^{(W)}\right)^{-1} \quad . \tag{8}$$

Since the nonresonant transfer rate is much less than the resonant one, i.e. $P_2^{(N)} \ll P_\pm^{(W)}$, the value of $n_2^{(s)}$ is close to unity.

We have numerically solved the stationary Schrödinger equation in the coordinate representation with the confining potential $V(x)$ shown in Fig. 1. For the method of solution, the dependence of $V(x)$ on the chemical composition of the well and effective mass m^* adopted in the calculations, see Ref. 5.

As an example, we consider the double well system (see Fig. 1) AW barrier/W well/WN barrier/N well/NB barrier with the widths equal to 100/19/8/14.5/100 nm, all the barriers being $Al_{0.1}Ga_{0.9}As$, which corresponds to the well depth $U_0 = 77.5$ meV. The solution yields the dependence of the excited level detuning $\epsilon_{43} = 2.56(E - 6.4)$ meV, where E is the bias field in kV/cm; the aligning electric field is $E_0 = 6.4$ kV/cm. For the aligning field, the solution gives the energy levels (meV) $\epsilon_1 = 4.7$, $\epsilon_2 = 15.9$, $\epsilon_- = 40.9$ and $\epsilon_+ = 43.9$; the tunneling amplitude $\tau = 1.5$ meV; the dipole matrix elements $d_{+1}/e = 2.4$ nm, $d_{-1}/e = -3.0$ nm with e as the elementary charge; and the localization probabilities $P_1^{(N)} = 0.98$, $P_2^{(W)} = 0.99$, $P_-^{(N)} = 0.58$ and $P_+^{(N)} = 0.42$. From the last set of data we see that the state $|1\rangle$ is, in fact, localized in the N well and $|2\rangle$ in the W well, while the $|+\rangle$ and $|-\rangle$ states are almost evenly delocalized over both the wells, as assumed above.

The transition rate γ_2 with $P_2^{(N)} = 0.01$ (see above) is very small with respect to γ_3, which ensures a high saturated probability (8) $n_2^{(s)} \approx 0.99$, low optical excitation rates $w^{(s)}$ needed to achieve saturation of the $|2\rangle$ state, $w^{(s)} \sim \gamma_2 \ll \gamma_\pm$, and comparatively long lifetime $t_c = \gamma_2^{-1}$ of the transferred charge after switching off the radiation. In practical terms, the typical decay rate of the excited states is $\gamma = 10^{12}$ s^{-1} = 0.66 meV, which yields $t_c = 0.1$ ns. For the linewidth of ~ 2 meV characteristic of QWEST and the dipole elements given above, the saturation light intensity $I_s = \epsilon_{\pm 1}\gamma_2/\sigma_\pm$ can be estimated as $I_s \sim 60$ kW/cm^2.

Besides the data shown above, the computation provides escape rates γ_{Bi} from the $|i\rangle$ states in the double well to the B region (Fig. 1b), i.e. in the direction of the potential drop. As expected, the largest of the obtained rates are those for the excited states, $\gamma_{B-} = 1.8$ μeV and $\gamma_{B+} = 1.1$ μeV. These escape rates play the role of the rate constants for a parasitic process of the light-induced leak from the quantum well. However, comparing $\gamma_{B\pm}$ to the tunneling amplitude $\tau = 1.5$ meV and also to the rates $\gamma_{2\pm} \sim 0.3$ meV of the population of the $|2\rangle$ state from $|\pm\rangle$, we arrive at the conclusion that the escape current is negligibly small with respect to the interwell tunneling current, and can cause only a very small positive charging of the well system as a whole without affecting the counter-field electron transfer.

The mean transfer quantum yield $\bar{Q}$ as a function of the bias electric field E calculated from Eqs. (5) and (7) for $\gamma_3 = \gamma_4$ is shown in Fig. 2 by a solid line. As one can see, Q has a rather sharp resonance at the field $E = 6.4$ kV/cm, which exactly corresponds to alignment of the excited levels in the two coupled wells. The maximum value is $\bar{Q}_{max} \approx 0.55$ and, as the computations show, it essentially does not depend upon the barrier width, which is a consequence of the coherency of the tunneling. As one can conclude from Eq. (7), the most favorable case for the counter-field transfer is not the simplest choice $\gamma_3 = \gamma_4$ as above, but rather $\gamma_4 \gg \gamma_3$, in which case $\bar{Q}$ can be close to unity.

The tunneling amplitude τ is an essential parameter, which determines whether the tunneling is coherent or not (see Secs. 3 and 4). This amplitude, which is equal to half the minimum value of the doublet splitting ϵ_{+-}, has been determined from the solution of the Schrödinger equation as a function of the width L_{WN} of the interwell (WN) barrier for the system of the above type with the widths $100/19/L_{WN}/14.5/100$ nm. The result is shown in Fig. 3, from which we can see that, in the range of L_{WN} considered, τ is an exponential function of L_{WN}, as expected.

The numerical solution given above illustrates basic features of the counter-field transfer effects, and, in principle, takes into account mixing between all the states in both the wells, and effect of the continuum states. However, the nature of the numerical solution is such that the analytical dependence of the effect on the parameters of the problem remain unclear. To elucidate this dependence, we will employ a conventional (see, e.g., Ref. 1) approximate approach based on the mixing of only two excited states, $|3\rangle$ and $|4\rangle$ and neglect of the overlap integral. The latter is equivalent to the orthogonality condition $\langle 3|4\rangle = 0$. The transfer

integral t in the notation of Ref. 1 is exactly our tunneling amplitude τ, and the approximation under consideration is nothing else but the tight-binding model with zero overlap in the basis of the two states $|3\rangle$ and $|4\rangle$.

The stationary Schrödinger equation in this basis is reduced to

$$(\epsilon_3 - \epsilon_\pm)\langle 3|\pm\rangle + \tau^*\langle 4|\pm\rangle = 0 \quad , \quad (\epsilon_4 - \epsilon_\pm)\langle 4|\pm\rangle + \tau\langle 3|\pm\rangle = 0 \quad , \tag{9}$$

with $\epsilon_\pm$ as eigenenergies. The solution of Eq. (9) has the familiar form $\epsilon_\pm = \frac{1}{2}\left[\epsilon_4 + \epsilon_3 \pm \left(\epsilon_{43} + 4|\tau|^2\right)^{1/2}\right]$, where $\epsilon_{43} \equiv \epsilon_4 - \epsilon_3$ is the energy mismatch of the excited levels. Also, the localization probabilities follow from Eq. (9) as

$$P_+^{(N)} = P_-^{(W)} = 1 - P_+^{(W)} = 1 - P_-^{(N)} = 4\frac{|\tau|^2}{\left[\epsilon_{43} + \left(\epsilon_{43}^2 + 4|\tau|^2\right)^{1/2}\right]^2 + 4|\tau|^2} \quad . \tag{10}$$

Substituting Eq. (10) into (2) we find the analytical expression for the transfer probability

$$n_2 = |G\tau|^2 \gamma_4\gamma_2^{-1}\left[\left(\epsilon_{43}^2 + 4\tau^2\right)(\Omega - \epsilon_{\pm 1})^2 + \frac{1}{4}\left(\gamma_4\epsilon_{\pm 3} - \gamma_3\epsilon_{\mp 3}\right)^2\right]^{-1} \tag{11}$$

Here the Rabi frequency $G = \mathbf{E}\mathbf{d}_{13}$ and, as usual, the notation ϵ_{ij} stands for $\epsilon_i - \epsilon_j$.

The mean quantum yield of transfer is found from Eqs. (7) and (10)

$$\bar{Q} = |\tau|^2(\gamma_3 + \gamma_4)\gamma_4\left[|\tau|^2(\gamma_3 + \gamma_4)^2 + \gamma_3\gamma_4\epsilon_{43}^2\right]^{-1} \quad . \tag{12}$$

As we see from Eq. (12), $\bar{Q}$ as a function of the level mismatch ϵ_{43} has the form of a symmetric peak with width $|\tau|(\gamma_4 + \gamma_3)(\gamma_3\gamma_4)^{-1/2}$ and maximum magnitude $\bar{Q}_{max} = (1 + \gamma_3/\gamma_4)^{-1}$. For the simplest choice $\gamma_3 = \gamma_4$, using the dependence $\epsilon_{43} = 2.56(E - 6.4)$ meV (see above), the mean quantum yield (12) is plotted in Fig. 2 as a function of E by the dashed line. We see that both in magnitude and form a simple analytical formula (12) agrees well with the result of the complete numerical calculation (Fig 2, solid line). This shows good applicability of the truncated-basis tight-binding approach used above to derive Eq. (12).

As mentioned above, $\bar{Q}_{max} = 0.5$ for $\gamma_3 = \gamma_4$, and $\bar{Q}_{max} \to 1$ for $\gamma_4 \gg \gamma_3$. The values of $\bar{Q}_{max}$ do not depend on the tunneling amplitude τ nor, consequently, on the barrier width. This is because of the coherent quantum tunneling assumed above. A high quantum yield of transfer demonstrated above and its dependence on the relaxation constant ratio deserves a

physical interpretation. The electron transfer counter to the electric field force is based on the quantum-mechanical delocalization of an electron over both the wells. This delocalization counterplays the electric field force and dominates in the case of realistic fields, where the above approximation is valid. As a result of the quantum delocalization, the electron can be found in the W well with a 50 percent probability. The relaxation in the W well with rate γ_4 causes the electron to get localized in this well, i.e. transferred against the field force. The relaxation in the N well with the rate γ_3 brings the electron back to the ground state, i.e. is a parasitic process. Therefore, $\bar{Q} \approx 1$ for $\gamma_4 \gg \gamma_3$.

3. EXCITATION AND ELECTRON TRANSFER IN DENSITY MATRIX FORMALISM

3.1. Basic equations

In the previous section we have described the electron excitation kinetics and counter-field transfer using the Schrödinger equation formalism. Such an approach is adequate for the coherent mechanism of the electron tunneling. The main drawback of this approach is the neglect of the polarization relaxation processes, which tend to destroy the coherence of tunneling. Below we present a general theory based on the density matrix approach, which allows one to describe the full range of the interwell tunneling regimes from completely coherent in the case of small polarization relaxation rate to the opposite case of completely stepwise for strong polarization relaxation. The simplifying feature of our approach is the use of the tight-binding model in the restricted basis of the states in isolated wells $|1\rangle, |2\rangle, |3\rangle, |4\rangle$ (see Sec. 2) and of the relaxation constant model for the relaxation term in the equation of motion for the density matrix (see below).

We start with the Hamiltonian of the system in the form $H = \sum_i \epsilon_i a_i^\dagger a_i + \sum_{ij} V_{ij} a_i^\dagger a_j$, where $a^\dagger$ and a are the electron creation and annihilation operators, with $i, j = 1, 2, 3, 4$. The one-electron operator V describes interaction with the electromagnetic field and electron interwell tunneling, and its independent nonzero elements are $V_{31} = -\mathbf{d}_{31}\left(\mathbf{E}e^{-i\Omega t} + \text{c.c.}\right)$, $V_{43} = \tau$. The one-electron density matrix r is defined as $r_{ij} = \left\langle a_j^\dagger a_i \right\rangle$. Its diagonal matrix elements are the population probabilities $n_i \equiv r_{ii}$.

The equation of motion for r can be obtained in the usual way by commuting the pair operator $a_j^\dagger a_i$ with the Hamiltonian and adding the relaxation term. This has the well-known

form

$$\frac{\partial r}{\partial t} = \imath\,[r, \epsilon + V] - R \quad , \tag{13}$$

where the one-electron energy operator ϵ is defined as $\langle i\,|\epsilon|\,j\rangle = \epsilon_i \delta_{ij}$. and R is the relaxation operator. In the low-temperature case, i.e. for neglect of thermal activation. the diagonal part of R describes spontaneous decays from higher- to lower-lying levels, and in the the model of relaxation constants has the form

$$R_{ii} = n_i \sum_{j\ (j<i)} \gamma_{ji} - \sum_{j\ (j>i)} \gamma_{ij} n_j \quad , \tag{14}$$

where γ_{ij} is the rate constant for spontaneous decay $|j\rangle \to |i\rangle$.

In what follows, we will neglect direct relaxation transitions which involve nonresonant interwell tunneling, $|3\rangle \to |2\rangle$ and $|4\rangle \to |1\rangle$, on the ground of small probability of nonresonant tunneling with respect to the resonant one. The rates of the above processes are negligible with respect to the rates of the collateral two-step processes involving the resonant tunneling, $|3\rangle \to |4\rangle \to |2\rangle$ and $|4\rangle \to |3\rangle \to |1\rangle$, which will be taken into account. Such a neglect is equivalent to the assumption of local character of the relaxation [see the discussion preceding Eq. (5)]. However, the nonresonant tunneling process $|2\rangle \to |1\rangle$ should be included despite its small rate, because there is no resonant process to compete with it. Thus, the following decay rate constants should only be taken into consideration: $\gamma_3 \equiv \gamma_{13}$, $\gamma_4 \equiv \gamma_{24}$, $\gamma_2 \equiv \gamma_{12}$. These rate constants have the same meaning as in Eq. (5).

The nondiagonal part of R describes the polarization relaxation and in the model under consideration is given by

$$R_{ij} = \Gamma_{ij} r_{ij} \quad , \qquad \Gamma_{ij} = \frac{1}{2}\,(\gamma_i + \gamma_j) + \bar{\Gamma}_{ij} \quad , \tag{15}$$

where $\bar{\Gamma}_{ij} \geq 0$ is the pure dephasing term.

Let us introduce, in the usual way, the density matrix in the interaction representation $\rho = \exp(-\imath\epsilon t) r \exp(\imath\epsilon t)$. The equation of motion for ρ follows from Eq. (13),

$$\frac{\partial \rho}{\partial t} = \imath\,[\rho, U] - S \quad . \tag{16}$$

Here $U \equiv \exp(\imath\epsilon t) V \exp(-\imath\epsilon t)$ and $S \equiv \exp(\imath\epsilon t) R \exp(-\imath\epsilon t)$ are the interaction and relaxation operators in the interaction representation. The diagonal part of S obviously coincides with

that of R as given by Eq. (14). The nondiagonal part of R is similar to Eq. (15) with the substitution ρ_{ij} for r_{ij}

The equations for the density matrix elements follow from Eq. (16) taking Eqs. (14)-(15) into account:

$$\begin{aligned}
\frac{\partial n_1}{\partial t} &= -2\mathbf{Im}\left[\rho_{13} V_{31} \exp\left(\imath\epsilon_{31} t\right)\right] + \gamma_2 n_2 + \gamma_3 n_3 \quad , \\
\frac{\partial n_2}{\partial t} &= -\gamma_2 n_2 + \gamma_4 n_4 \quad , \\
\frac{\partial n_3}{\partial t} &= 2\mathbf{Im}\left[\rho_{13} V_{31} \exp\left(\imath\epsilon_{31} t\right)\right] - \gamma_3 n_3 + 2\mathbf{Im}\left[\rho_{43} \tau^* \exp\left(-\imath\epsilon_{43} t\right)\right] \quad , \\
\frac{\partial n_4}{\partial t} &= -2\mathbf{Im}\left[\rho_{43} \tau^* \exp\left(-\imath\epsilon_{43} t\right)\right] - \gamma_4 n_4 \quad , \\
\frac{\partial \rho_{13}}{\partial t} &= \imath\left(n_1 - n_3\right) V_{31}^* \exp\left(-\imath\epsilon_{31} t\right) + \imath\rho_{14} \tau \exp\left(\imath\epsilon_{43} t\right) - \Gamma_{13}\rho_{13} \quad , \\
\frac{\partial \rho_{14}}{\partial t} &= -\imath\rho_{43}^* V_{31}^* \exp\left(-\imath\epsilon_{31} t\right) + \imath\rho_{13} \tau^* \exp\left(-\imath\epsilon_{43} t\right) - \Gamma_{14}\rho_{14} \quad , \\
\frac{\partial \rho_{43}}{\partial t} &= \imath\rho_{14}^* V_{31}^* \exp\left(-\imath\epsilon_{31} t\right) + \imath\left(n_4 - n_3\right) \tau \exp\left(\imath\epsilon_{43} t\right) - \Gamma_{43}\rho_{43} \quad .
\end{aligned} \tag{17}$$

The system of equations (17) is exact for the model under consideration. Below we adopt the resonant approximation, which is also synonymously called the Rotating-Wave Approximation (RWA). Applicability of this approximation is well established for optical fields not very strong. Technically, RWA is equivalent to taking into account only the terms containing slowly-oscillating temporal exponentials in Eq. (17). Doing so, we can explicitly determine the temporal dependence of the polarizations,

$$\rho_{13} = \bar{\rho}_{13} \exp\left[\imath\left(\Omega - \epsilon_{31}\right) t\right] \quad , \quad \rho_{14} = \bar{\rho}_{14} \exp\left[\imath\left(\Omega - \epsilon_{41}\right) t\right] \quad , \quad \rho_{43} = \bar{\rho}_{43} \exp\left[\imath\epsilon_{43} t\right] \quad , \tag{18}$$

and find the system of equations with constant coefficients

$$\begin{aligned}
\frac{\partial n_1}{\partial t} &= -2\mathbf{Im}\left(\bar{\rho}_{13} G\right) + \gamma_2 n_2 + \gamma_3 n_3 \quad , & \frac{\partial n_2}{\partial t} &= -\gamma_2 n_2 + \gamma_4 n_4 \quad , \\
\frac{\partial n_3}{\partial t} &= 2\mathbf{Im}\left(\bar{\rho}_{13} G\right) - \gamma_3 n_3 + 2\mathbf{Im}\left(\bar{\rho}_{43} \tau^*\right) \quad , & \frac{\partial n_4}{\partial t} &= -2\mathbf{Im}\left(\bar{\rho}_{43} \tau^*\right) - \gamma_4 n_4 \quad , \\
\frac{\partial \bar{\rho}_{13}}{\partial t} &= \imath G^* \left(n_1 - n_3\right) + \imath\tau\bar{\rho}_{14} - g_{13}\bar{\rho}_{13} \quad , & \frac{\partial \bar{\rho}_{14}}{\partial t} &= -\imath G^* \bar{\rho}_{43}^* + \imath\tau^* \bar{\rho}_{13} - g_{14}\bar{\rho}_{14} \quad , \\
\frac{\partial \bar{\rho}_{43}}{\partial t} &= \imath\tau\left(n_4 - n_3\right) + \imath G^* \bar{\rho}_{14}^* - g_{43}\bar{\rho}_{43} \quad ,
\end{aligned} \tag{19}$$

where the notations are introduced [G is defined after Eq. (11)]

$$g_{13} \equiv \Gamma_{13} + \imath\left(\Omega - \epsilon_{31}\right) \quad , \quad g_{14} \equiv \Gamma_{14} + \imath\left(\Omega - \epsilon_{41}\right) \quad , \quad g_{43} = \Gamma_{43} + \imath\epsilon_{43} \quad . \tag{20}$$

3.2. Temporal dynamics

The fundamental system of equations (19) describes both the temporal evolution and stationary levels of the electron polarization and population numbers. Beginning with dynamics, the simplest effect is known to be the quantum beats: the system is excited with a short pulse of light and, after the pulse is over, the population numbers and polarizations are changing in time, in some cases in an oscillating manner. Such observation conditions are in a close correspondence with the experimental study of Ref. 8.

The kinetics of the quantum beats is described by Eq. (19), where $G = 0$. In this case, we see that the equations related to the tunneling-connected states $|3\rangle$ and $|4\rangle$ decouple from the rest of equations (19), forming a closed system

$$\frac{\partial n_3}{\partial t} = -\gamma_3 n_3 + 2\mathbf{Im}(\tau^* \bar{\rho}_{43}) \ , \quad \frac{\partial n_4}{\partial t} = -\gamma_4 n_4 - 2\mathbf{Im}(\tau^* \bar{\rho}_{43}) \ , \qquad \frac{\partial \bar{\rho}_{43}}{\partial t} = \imath\tau\,(n_4 - n_3) - g_{43}\bar{\rho}_{43} \ . \tag{21}$$

The solution of this system is given by a superposition of exponentials $e^{\lambda_n t}$ with the coefficients, which can be found from the initial conditions determined by the excitation process. However, the corresponding characteristic exponents λ_n are the eigenvalues of Eq. (21), which do not depend on the initial conditions.

The system (21) is equivalent to four real equations (the matrix element $\bar{\rho}_{43}$ is complex). The corresponding characteristic equation is fourth-order and yields analytical expressions for the four eigenvalues λ_n. However, these expressions are too complicated. Therefore, we will assume simplifying conditions, which do not affect the general properties of the solution. These conditions are zero level mismatch ($\epsilon_{43} = 0$) and equal decay rates of the excited levels ($\gamma_3 = \gamma_4$). In this case, we obtain the four characteristic exponents λ_1, λ_2, λ_+, λ_- to be

$$\lambda_1 = -\gamma_3 \ , \quad \lambda_2 = -\Gamma_{43} \ , \quad \lambda_\pm = -\frac{1}{2}(\gamma_3 + \Gamma_{43}) \pm \left(\frac{1}{4}\bar{\Gamma}_{43}^2 - 4\,|\tau|^2\right)^{1/2} \ . \tag{22}$$

We can see from Eq. (22) that the first two exponents correspond to purely decaying (aperiodical) kinetics. The two other exponents $\lambda_\pm$ may have an imaginary part and, consequently, describe an oscillating evolution depending on the relation between the pure dephasing term $\bar{\Gamma}_{43}$ [cf. Eq. (15)] and the tunneling amplitude τ. Namely, if $\bar{\Gamma}_{43} < 4\,|\tau|$, then the oscillations of the populations n_3, n_4 and polarization $\bar{\rho}_{43}$ with the frequency $\omega_b = \left(4\,|\tau|^2 - \frac{1}{4}\bar{\Gamma}_{43}^2\right)^{1/2}$

are possible, depending on the initial conditions. Let us emphasize that ω_b does not depend whatsoever on the population decay rates γ_i.

Physically, the oscillations considered above mean coherent tunneling transitions of an electron from one quantum well to the other and back. These oscillations decay with the rate $\gamma_3 + \bar{\Gamma}_{43}/2$ depending on both the population decay constant γ_3 and the dephasing rate $\bar{\Gamma}_{43}$. Such coherent oscillations have been suggested in Ref. 7 and observed experimentally in Ref. 8. However, in the theoretical description of Refs. 7 and 8, the dephasing has not been taking into account. If the dephasing is negligible ($\bar{\Gamma}_{43} \ll |\tau|$), the frequency ω_b of beats is equal to the doublet splitting, and for the case of exactly aligned levels we have $\omega_b = 2|\tau|$, in accord with Refs. 7 and 8. However, in a practical situation, the dephasing is not small, and $\omega_b < 2|\tau|$. As the results obtained above show, the dephasing relaxation rate $\bar{\Gamma}_{43}$ is a very important parameter, which not only determines the values of the frequency and decay rate of oscillations, but their very existence.

3.3. Stationary solutions

The stationary solution of Eq. (19) can be obtained in a straightforward manner. The expressions for the population probabilities of the excited levels are

$$\begin{aligned} n_3 = &\Big[c(b+\gamma_4) - a(a+\gamma_4)\Big]\Big\{c\left[b(3+\gamma_4/\gamma_2)+2\gamma_4\right] + \\ &\gamma_3\gamma_4 + b(\gamma_3+\gamma_4) + a\left[\gamma_3(1+\gamma_4/\gamma_2) - a(3+\gamma_4/\gamma_2) - 3\gamma_4\right]\Big\}^{-1} \quad , \\ n_4 = &\Big[a(\gamma_3 - a) + cb\Big]\Big\{c\left[b(3+\gamma_4/\gamma_2)+2\gamma_4\right] + \\ &\gamma_3\gamma_4 + b(\gamma_3+\gamma_4) + a\left[\gamma_3(1+\gamma_4/\gamma_2) - a(3+\gamma_4/\gamma_2) - 3\gamma_4\right]\Big\}^{-1} \quad , \end{aligned} \tag{23}$$

where the notations are introduced

$$\begin{aligned} a \equiv 2|\tau|^2|G|^2 \mathbf{Re}\left(f^{-1}\right) \quad , \quad b \equiv 2|\tau|^2 \mathbf{Re}\left[\left(g_{13}g_{14} + |\tau|^2\right) f^{-1}\right] \quad , \\ c \equiv 2|G|^2 \mathbf{Re}\left[\left(g_{43}^* g_{14} + |G|^2\right) f^{-1}\right] \quad , \quad f \equiv g_{43}\left(g_{13}g_{14} + |\tau|^2\right) + g_{13}|G|^2 \quad . \end{aligned} \tag{24}$$

As follows from from the second of the equations (19), the probability n_2 of the electron transfer is simply related to n_4 by

$$n_2 = \gamma_4 \gamma_2^{-1} n_4 \quad . \tag{25}$$

The expressions (23) are exact. However, they are somewhat cumbersome and difficult to analyze. In particular, it is difficult to see from Eq. (24) how the Schrödinger approach results (see Sec. 2) can be reproduced. Therefore, prior to giving numerical examples, we shall consider simplifying limiting cases, restricting ourselves to an optically nonsaturated regime, $|G| \ll \gamma_i,\ |\tau|$. Assuming this, we obtain from Eq. (23) closed expressions for the population numbers

$$n_3 = \frac{2|G|^2}{X}\left\{ \left[|\tau|^2 + \Gamma_{13}\Gamma_{14} - (\Omega - \epsilon_{31})(\Omega - \epsilon_{41})\right]\left[|\tau|^2\Gamma_{43}(2\Gamma_{14} - \gamma_4) + \gamma_4\Gamma_{14}(\Gamma_{43}^2 + \epsilon_{43}^2)\right] + \right.$$
$$\left. \left[\Gamma_{13}(\Omega - \epsilon_{41}) + \Gamma_{14}(\Omega - \epsilon_{31})\right]\left[|\tau|^2(2\Gamma_{43}(\Omega - \epsilon_{41}) - \gamma_4\epsilon_{43}) + \gamma_4(\Omega - \epsilon_{41})(\Gamma_{43}^2 + \epsilon_{43}^2)\right]\right\} ,$$

$$n_4 = \frac{2|\tau|^2|G|^2}{X}\left\{ \left[|\tau|^2 + \Gamma_{13}\Gamma_{14} - (\Omega - \epsilon_{31})(\Omega - \epsilon_{41})\right]\Gamma_{43}(2\Gamma_{14} + \gamma_3) + \right.$$
$$\left. \left[\Gamma_{13}(\Omega - \epsilon_{41}) + \Gamma_{14}(\Omega - \epsilon_{31})\right]\left[\gamma_3\epsilon_{43} + 2\Gamma_{43}(\Omega - \epsilon_{41})\right]\right\} , \tag{26}$$

where the notation is used

$$X \equiv \left\{ \left[|\tau|^2 + \Gamma_{13}\Gamma_{14} - (\Omega - \epsilon_{31})(\Omega - \epsilon_{41})\right]^2 + \left[\Gamma_{13}(\Omega - \epsilon_{41}) + \Gamma_{14}(\Omega - \epsilon_{31})\right]^2\right\} \times$$
$$\left[2|\tau|^2\Gamma_{43}(\gamma_3 + \gamma_4) + \gamma_3\gamma_4(\Gamma_{43}^2 + \epsilon_{43}^2)\right] . \tag{27}$$

The populations (26) are proportional to $|G|^2$, i.e. to the light intensity, as expected.

From Eq. (26) we can see how to reproduce the results of Sec. 2. If the polarization relaxation rates are much smaller than the tunneling amplitude,

$$\Gamma_{13},\ \Gamma_{14},\ \Gamma_{43} \ll |\tau| , \tag{28}$$

the denominator X (27) in Eq. (26) becomes nearly zero for $\Omega = \epsilon_{+1}$ or $\Omega = \epsilon_{-1}$, where $\epsilon_{\pm}$ are the energies of the doublet levels. In this case, each of the populations n_3 and n_4 as a function of frequency has two nonoverlapping peaks centered at the frequencies $\epsilon_{\pm 1}$. In the vicinities of these peaks, the expression for n_4 has the form

$$n_4 = \frac{2|\tau|^2|G|^2(\Gamma_{14}\epsilon_{\pm 3} - \Gamma_{13}\epsilon_{\mp 3})(\gamma_3\epsilon_{43} - 2\Gamma_{43}\epsilon_{\mp 3})}{\left[(4|\tau|^2 + \epsilon_{43}^2)(\Omega - \epsilon_{\pm 1})^2 + (\Gamma_{14}\epsilon_{\pm 3} - \Gamma_{13}\epsilon_{\mp 3})^2\right]\left[2|\tau|^2\Gamma_{43}(\gamma_3 + \gamma_4) + \epsilon_{43}^2\gamma_3\gamma_4\right]} . \tag{29}$$

Taking Eq. (25) into account, we conclude that Eq. (29) agrees with the result (11) of the Schrödinger equation approach only if, in addition to the condition (28), pure dephasing is

negligible with respect to the population relaxation,

$$\bar{\Gamma}_{14} \ll \gamma_4 \ , \quad \bar{\Gamma}_{13} \ll \gamma_3 \ , \quad \bar{\Gamma}_{43} \ll \gamma_4 + \gamma_3 \ . \tag{30}$$

Inapplicability of the Schrödinger equation approach in the presence of the dephasing is evident if consider the mean quantum yield $\bar{Q}$ (6), which can be calculated from Eqs. (25) and (29),

$$\bar{Q} = 2\,|\tau|^2\,\Gamma_{43}\gamma_4\left[2\Gamma_{43}\,|\tau|^2\,(\gamma_3+\gamma_4)+\gamma_3\gamma_4\epsilon_{43}^2\right] \tag{31}$$

in comparison with the corresponding result (12). Note that the condition (28) may be realistic, but (30) is normally not the case (see below). Therefore, taking into account the polarization relaxation with the use of the density matrix techniques, is essential.

3.4. Numerical illustrations

In this subsection we numerically illustrate properties of the optical excitation in the coupled quantum wells, with emphasis on the counter-field electron transfer. We aim to elucidate the effect of the polarization relaxation on the electron excitation and transfer.

The exact expressions for the population probabilities n_3, n_4 of the excited levels are given by Eq. (23). The probability n_2 of the electron transfer in accordance with Eq. (25) simply copies n_4. Since the expressions (23) crucially depend on the polarization relaxation constants Γ_{13}, Γ_{14}, Γ_{43}, we begin with estimating these constants.

Experimentally, the polarization relaxation constant is found as the width of the optical absorption line under nonsaturated excitation conditions. Using such an approach, it has been established in Ref. 14 that at the temperatures $T \leq 100$ K and the transition energy $\epsilon \leq 100$ meV, the transition width Γ does not significantly depend on T, and $\Gamma/\epsilon \approx 0.03$. These data show that the contribution of the optical phonons to the polarization relaxation under the conditions used is small.[14] The optical phonon contribution will be even smaller in the absence of optical phonon emission, which is the case for $\epsilon_{31} < \omega_o$, where ω_o is the optical phonon frequency. This condition is satisfied for the system under consideration.

With the optical phonons excluded, the remaining mechanism of the dephasing is based on the fluctuation of plus-minus one monolayer in the width of the well. This mechanism is also supported[15] by the experimental data on the interband transitions in quantum wells. Assuming this mechanism, we arrive at a simple estimate $\bar{\Gamma}/\epsilon \approx 2\delta a/a$, where a is the well width and δa is

its fluctuation, $\delta a \approx 0.3$ nm. In our case, e.g. for the N well, $a = 14.4$ nm and $\bar{\Gamma}/\epsilon \approx 0.04$. For a crude estimate, the agreement with the experimental value is reasonable. For the example considered, this estimate yields $\bar{\Gamma}_{13}$, $\bar{\Gamma}_{14} \approx 1.5$ meV. In the absence of optical phonon emission, a typical lifetime of the intersubband transition is ~ 3 ps. This yields the decay constants γ_3, $\gamma_4 \approx 0.2$ meV. Thus, the dephasing contributions to the polarization relaxation constants dominate, in contrast to the applicability condition (30) of the Schrödinger equation approach.

To estimate the interwell polarization relaxation rate Γ_{43}, we notice that the fluctuation of the excited level energies ϵ_3 and ϵ_4 are always greater than those of the the ground states ϵ_1, ϵ_2. In this case, assuming the fluctuations in the different wells to be independent, we obtain a simple relation $\bar{\Gamma}_{43} = \left(\bar{\Gamma}_{13}^2 + \bar{\Gamma}_{14}^2\right)^{1/2}$, which will be used below.

The effect of the polarization relaxation on the electron excitation can be traced in Fig. 4. We can see in Fig. 4a that in the case of a weak dephasing ($\Gamma_{13} = \Gamma_{14} = 0.1$ meV), the excitation contours are two almost separate peaks, which, as can easily be verified, are positioned at the transitions frequencies $\tau_\pm$ of the doublet levels. The asymmetry of the excitation contour is due to nonzero level mismatch ϵ_{43}.

We emphasize that near the peak maxima $n_4 \sim n_3$, which means that the electron transfer counter to the electric field force occurs with a high probability, an electron is excited by the light to the $|3\rangle$ state, but appears with close or even greater probability in the $|4\rangle$ state localized in the other well. Using Eq. (25), we can make sure that in the spectral maxima $n_2 \approx 1$, i.e. the populations are saturated. At the same time, the parameter, which governs the polarization saturation, $|G|^2 / \Gamma_{13}^2 \ll 1$. This means, in particular, an absence of field broadening and low probability of excitation into the continuum.

With an increase of the dephasing rate (see Fig. 4b,c), the spectral peaks are broadened and overlap. However, the population number n_4 and, consequently, the transfer probability n_2 (25) do not considerably diminish. This witnesses that the counter-field transfer effect persists even for relatively strong dephasing. For $\Gamma_{13} = \Gamma_{14} = 10$ meV, the doublet structure is completely absent, and the absorption contour is symmetrical and centered at the frequency ϵ_{31} of the transition in the isolated narrow well (Fig. 5c). This means that the electron is first excited within the N well and then tunnels into the W well, i.e. the tunneling is incoherent.

The effect of the polarization relaxation is even less evident for the case of nonequal dephasing rates in the two wells shown in Fig. 5. With an increase of the dephasing in the

wide well, the peaks begin to broaden (Fig. 5a, cf. Fig. 4a), but then this broadening stops (Fig. 5b) and reverses: for strong relaxation we observe a single narrow peak centered at the transition frequency ϵ_{31} of an isolated narrow well (Fig. 5c). Again, this fact witnesses that the tunneling is incoherent. The narrowing of the absorption contour for the case of strong dephasing is a counterpart of the well known spectroscopic phenomenon of the spectral line collapse. This narrowing can be understood from the following arguments. With an increase of the dephasing in the W well, this well behaves like an overdamped resonator. Such a resonator is known to decouple from a high-quality resonator, which is the W well. In such a way, a well with a strong polarization relaxation does not considerably perturb the other well.

To focus on the effect of counter-field electron transfer, let us consider Fig. 6, in which the maximum (in the light frequency) probability of this transfer is shown as a function of the tunneling amplitude τ. Note that for the double-well system under consideration, the magnitude of τ is simply related to the thickness L_{WN} of the interwell barrier (see Fig. 3).

In the case of low-to-intermediate optical saturation ($|G| = 0.2$), we see from Fig. 6a that for $\tau \ll \bar{\Gamma}_{13}$ the transfer probability strongly depend on τ, in fact $n_2 \propto |\tau|^2$. This a feature of a noncoherent electron transfer. With increase of τ, the probability n_2 levels off. The greater γ_{13}, the later this leveling takes place and the lower is the limiting magnitude of n_2. For the typical value $\tau \approx 1$ meV, the transfer probability is very high, $n_2 \approx 0.7$. Thus, the counter-field transfer effect is strong under the realistic conditions considered. For a high light intensity $|G| = 20$ meV (Fig. 6b), the transfer is completely saturated, $n_2 \approx 1$, in the coherent tunneling regime. However, there exists an essential difference with the intermediate-intensity case (Fig. 6a). Namely, the effect of the dephasing is opposite: the higher Γ_{13}, the higher n_2, and the sooner the saturation sets on. This counterintuitive feature stems from the field broadening, which prevails over the phase relaxation in this case.

4. DISCUSSION

This paper pursues two interrelated goals. The first is to give a theoretical description of a novel effect in asymmetric double quantum wells, namely, the electron transfer counter to the bias field. This transfer is based on the quantum-mechanical delocalization of the electron over the resonant states, which, in the case under consideration, prevails over the electric field force (note that the light itself does not exert any significant force). The second goal of the paper is to develop a theory which describes the kinetics of the electron excitation in coupled

quantum wells taking into account the polarization relaxation.

An approach based on the Schrödinger equation provides a comprehensive description of the problem. This is given in Sec. 2, where general expressions (2) for the electron transfer probability n_2 and (7) for the mean quantum yield $\bar{Q}$ of transfer are obtained [see also Eq. (12) and Fig. 2].

However, the Schrödinger equation approach is only valid in the absence of the polarization relaxation (dephasing), which always exists in real systems. This relaxation destroys quantum-mechanical coherence and, rigorously speaking, makes the stationary states of the electron nonexisting. Physically, the polarization relaxation originates from interaction of an electron with other parts of the system, in particular, with phonons and impurities or defects, which are not taken unto account in the Schrödinger equation. In this case, the density matrix technique is adequate. Such technique for the optical excitation of a double quantum well is developed in Sec. 3.

The free (i.e. in the absence of the optical field) time-dependent solution of Eq. (19) [see also Eq. (20)] gives the frequency of the quantum beats ω_b. In the presence of phase relaxation, this frequency does not coincide with the spacing of the excited state doublet, and is determined by the dephasing constant $\bar{\Gamma}_{43}$ but not the decay constants. If the phase relaxation is strong enough, $\bar{\Gamma}_{43} > 4|\tau|$, then the quantum beats disappear, completely replaced by a monotonic relaxation. The results discussed may be of interest for comparison with recent experiments of Ref. 8, in which quantum beats in the double wells have been observed.

In the stationary regime, closed analytical expressions (23) and (25) for the populations n_3 and n_4 of the excited states are obtained. The full range of the transition from a nearly coherent tunneling regime to an almost incoherent one can be traced in Figs. 4 and 5. For a weak polarization relaxation, the excitation profiles reveal a two-peak structure typical for the coherent tunneling. In this case, the optical wave plays the role of a probe field exciting the system to the doublet states $|\pm\rangle$. As the dephasing increases, the stationary states $|\pm\rangle$ are no longer a good zero-order approximation, and the interwell coupling becomes incoherent (stepwise): the first step is the excitation from the state $|1\rangle$ to $|3\rangle$ of the W well followed by the second step of the tunneling into the N well. In qualitative agreement with the above picture, with an increase of the dephasing, the double-peak structure disappears, replaced by a single peak centered at the transition frequency ϵ_{31}. If the dephasing in the two coupled

wells is increased in the same proportion, the excitation profiles are broadened (see Fig. 4c). An counter-intuitive feature appears in the case where the dephasing is increased only in the acceptor (W) well: eventually, a collapse of the spectral line takes place (see Fig. 5c).

To avoid possible misunderstanding, we recall that the form of the excitation profiles in Figs. 4 and 5 is obtained under the assumption that only the transitions from the ground state $|1\rangle$ in the N well are excited. These transitions are positioned on the energy scale to the right of the transitions in the W well. Therefore, in practice, the right parts ($\Omega \geq 30$ meV) of the excitation profiles should be close to the ones shown in Figs. 4 and 5, and the left parts may differ. However, for the nonsaturating optical excitation, only the transitions in the N well can occur, because only the $|1\rangle$ state in this well, as the overall ground state, is populated at low temperatures. Therefore, under these conditions, the excitation profiles are correctly given by Eq. (26) in the whole spectral region, predicting dependences similar to those of Figs. 4 and 5.

As discussed above, the phase relaxation drastically affects the spectral profiles of the optical excitation. Also, it is understandable *a priori* that the probability n_2 of the counter-field electron transfer diminishes with the increase of the dephasing because the transfer is a resonant effect, and the quality of the resonance is reduced by the polarization relaxation. A question remains to which degree n_2 is affected. The answer is contained in Fig. 6a: for moderate excitation intensities and the whole conceivable range of $\bar{\Gamma}_{13} = 0.1 - 10$ meV, the probability n_2 changes only by a factor of 0.3. Therefore, the transfer effect itself is rather stable with respect to the dephasing.

Let us discuss possible experimental observation of the counter-field electron transfer. This effect can be detected optically by monitoring changes of the intersubband absorption in the double well: as the transfer proceeds, the absorption band shifts to a lower frequency by the amount ϵ_{21}. Electrical detection of the transfer is also possible. In this case, external conductors should be in contact with the regions A and B in Fig. 1. However, achieving the regime of a stationary current in the external circuit is problematic, because in this case the barriers AW and NB should be penetrable for electrons. If so, the optical excitation, apart from bringing about the counter-field electron transfer, would also increase the rate of the electron escape from the N well to the B region, i.e. in the direction favored by the bias. Thus the counter-field transfer may be completely masked by this leak current.

We believe that the most reliable is the detection of the counter-field transfer based on

the capacitance coupling of the well to an external circuit. Such coupling is achievable even with the thick barriers AW and NB, thus excluding photoinduced leakage from the N well to B region discussed above.

In the case of the capacitance coupling, the regions A and B (Fig. 1), containing a dense electron gas, play the role of the capacitor plates. For the regime of zero current in the external circuit, the counter-field transfer of electrons induced by switching on of the light brings about an *increase* of the potential difference ΔU_{AB},

$$\Delta U_{AB} = 4\pi e\sigma n_2 \Delta x/\varepsilon \quad , \qquad \Delta x \equiv \int_{-\infty}^{\infty} \left[|\Psi_1(x)|^2 - |\Psi_2(x)|^2 \right] x \mathrm{d}x \quad , \tag{32}$$

where Ψ_i is the wave function of the $|i\rangle$ state, ε is the mean dielectric constant of the well material, σ is two-dimensional density of the electron gas in the well, and x has meaning of the characteristics distance of the charge transfer (for the example considered, $\Delta x = 24$ nm). We emphasize that $\Delta U > 0$ means that the photocurrent inside the well is directed *counter* to the potential drop.

Alternatively, if the capacitor is externally kept under a constant potential difference, then an exciting light pulse brings about a transient current in the external circuit *opposite* to the direction favored by the bias, the total transferred charge being $Q = eS\sigma n_2 \Delta x/L$, where L is the AB distance, and S is the illuminated area; $\Delta x/L \approx 0.1$ for the system considered.

We should point out the the theory presented above does not take into account the photoinduced electric fields. This condition can always be met if the density σ is low enough. In this case, of course, the potential change (32) is small. However, it is expedient to mention the probable qualitative effects of the photoinduced fields. The potential increase ΔU_{AB}, via changing the electric field inside the well, affects the photoexcitation and electron transfer. This is a feedback which can produce enhanced nonlinear optical responses, similar to ones observed in Ref. 6 for the interband transitions, and, possibly, an intrinsic optical bistability. We shall address these effects elsewhere.

The authors are grateful to B. D. McCombe for useful discussions. We acknowledge use of facilities of the Pittsburgh Supercomputing Center under grant PHY890020P. This work has been supported by the Office of Naval Research.

REFERENCES

* Also with Institute of Automation and Electrometry, Siberian Branch of the USSR Academy of Sciences, 630090 Novosibirsk, USSR.

1. Gerald Bastard, *Wave Mechanics Applied to Semiconductor Heterostructures* (Les Editions de Physique, Les Ulis, France, 1988).
2. R. Sauer, K. Thonke, and W. T. Tsang, Phys. Rev. Lett. **61**, 609 (1988).
3. B. Deveaud, F. Clerot, A. Chomette, A. Regreny, R. Ferreira, G. Bastard, and B. Sermage, Europhys. Lett. **11**, 367 (1990).
4. D. Y. Oberli, J. Shah, T. C. Damen, C. W. Wu, T. Y. Chang, D. A. B. Miller, J. E. Henry, R. F. Kopf, N. Sauer, and A. E. DiGiovanni, Phys. Rev. B **40**, 3028 (1989).
5. L. N. Pandey and T. F. George, J. Appl. Phys. **69**, 2711 (1991).
6. D. J. Leopold and M. M. Leopold, Phys. Rev. B **42**, 11147 (1990).
7. S. Luryi, Solid State Commun. **1988**, 787 (1990).
8. K. Leo, J. Shah, E. Göbel, T. Damen, S. Schmitt-Rink, and W. Schäfer, Phys. Rev. Lett. **66**, 201 (1991).
9. R. Ferreira, C. Delalande, H. W. Liu, G. Bastard, B. Etienne, and J. F. Palmier, Phys. Rev. B **42**, 9170 (1990).
10. M. G. W. Alexander, M. Nido, W. W. Ruhle, and K. Kohler, Phys. Rev. B **41**, 12295 (1990).
11. H. W. Liu, R. Ferreira, G. Bastard, C. Delande, J. F. Palmier, and B. Etienne, Phys. Rev. Lett. **54**, 2082 (1989).
12. H. C. Liu, M. Buchanam, and Z. R. Vasilevski, J. Appl. Phys. **68**, 3780 (1990).
13. A. Palevsky, F. Beltram, F. Capasso, L. Pfeifer, and K. W. West, Phys. Rev. Lett. **65**, 1929 (1990).
14. M. O. Manasreh, F. Szmulovich, D. V. Fischer, K. R. Evans, and C. E. Stutz, Appl. Phys. Lett. **57**, 1790 (1990).
15. W. S. Fu, G. R. Olbright, A. Owyoung, J. F. Klemm, R. M. Biefield, and G. R. Hadley, Appl. Phys. Lett. **57**, 1404 (1990).

FIGURE CAPTIONS

Fig. 1. Coupled wide (W) and narrow (N) quantum wells (a - in the absence of bias, b - in the presence, where the excited levels are aligned). Schematic of the confining potential, energy levels, and radiative (wavy arrow) and nonradiative (dashed arrows) transitions. The regions A and B containing a dense electron gas serve as electrodes for the capacitance coupling of the double well to an external circuit. The insulating barriers AW and NB are supposed to be thick and high enough to exclude considerable tunneling through them (see the text).

Fig. 2. Quantum yield Q of the electron transfer counter to the field force as a function of the electric field E applied to the double well. The data are obtained from numerical computation according to Eq. (7) (solid line) and with the use of analytical formula (12) (dashed line).

Fig. 3. Tunneling amplitude τ (meV) as a function of the central barrier width L_{WN} (nm) in the double logarithmic scale.

Fig. 4. Population numbers n_3 (solid line) and and n_4 (dashed line) of the excited levels as functions of the exciting light frequency Ω (meV) for the dephasing constants shown in the graphs. The dephasing relaxations in the two coupled wells are assumed equal, $\bar{\Gamma}_{13} = \bar{\Gamma}_{14}$. The other relevant parameters are $|G| = 0.2$ meV, $\gamma_3 = \gamma_4 = 0.2$ meV, $\Gamma_2 = 0.006$ meV, and $\epsilon_{43} = 1$ meV. The double-well system under consideration is described in the text.

Fig. 5. The same as Fig. 4, but the dephasing in the narrow well is the same for all the graphs shown, $\bar{\Gamma}_{13}$ =const, and dephasing in the wide well is increasing, $\bar{\Gamma}_{14} = 0.1$, 1, 10 meV.

Fig. 6. Transfer probability n_2 calculated in its spectral maximum as a function of the tunneling amplitude τ for the dephasing rates $\gamma_{13} = 0.1$, 1, 10 meV, and the Rabi frequencies $G = 0.2$, 20 meV, as shown on the graphs. Other parameters: $\gamma_{14} = \gamma_{13}$, the decay rates $\gamma_3 = \gamma_4 = 0.2$ meV, $\gamma_2 = 0.006$ meV, and the level mismatch $\epsilon_{43} = 0$.

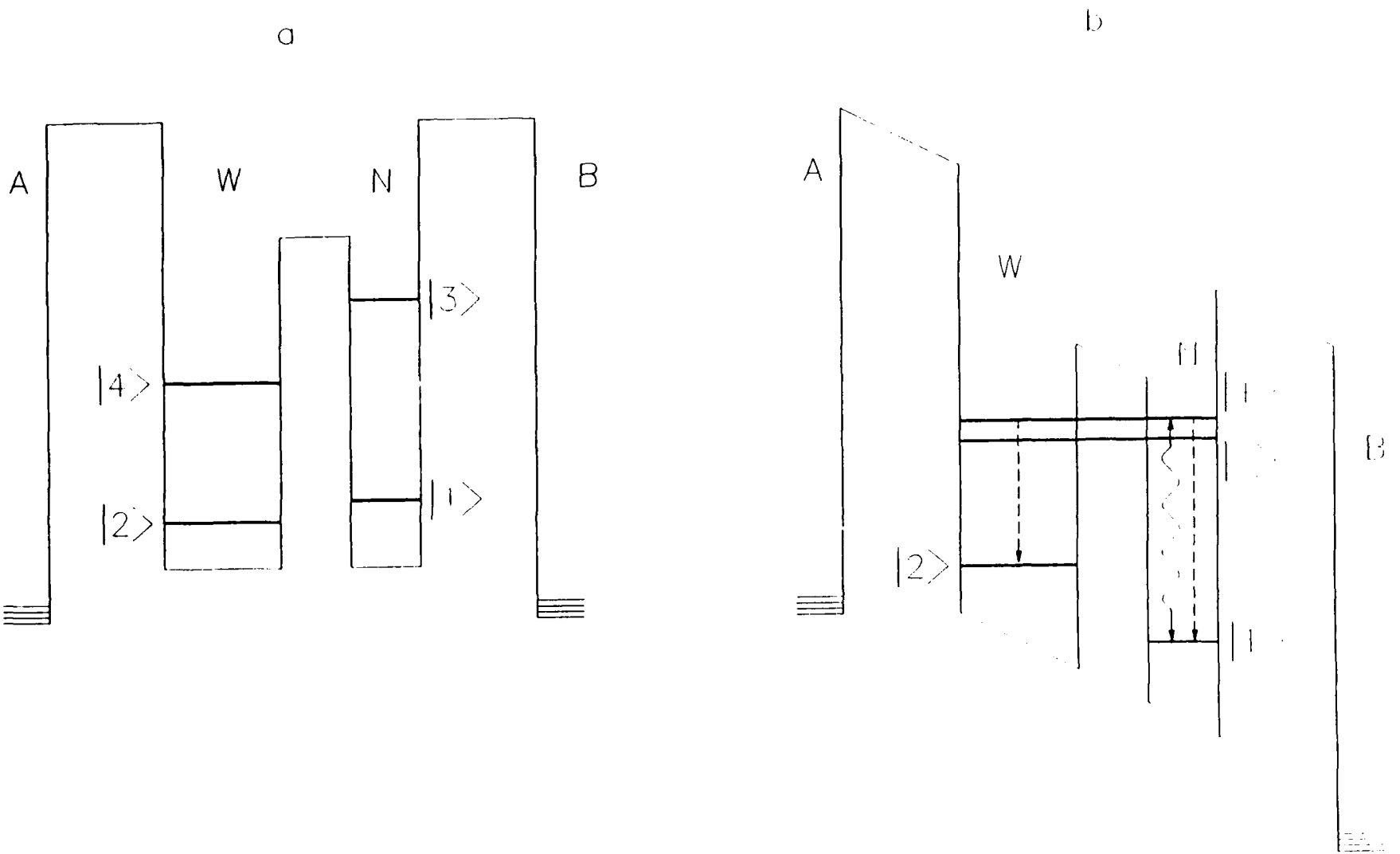

Fig. 1

Marc I. Stockman "Kinetics of intersubband ..."

Mark I. Stockman et all "Kinetics of intersubband..."

Fig. 2

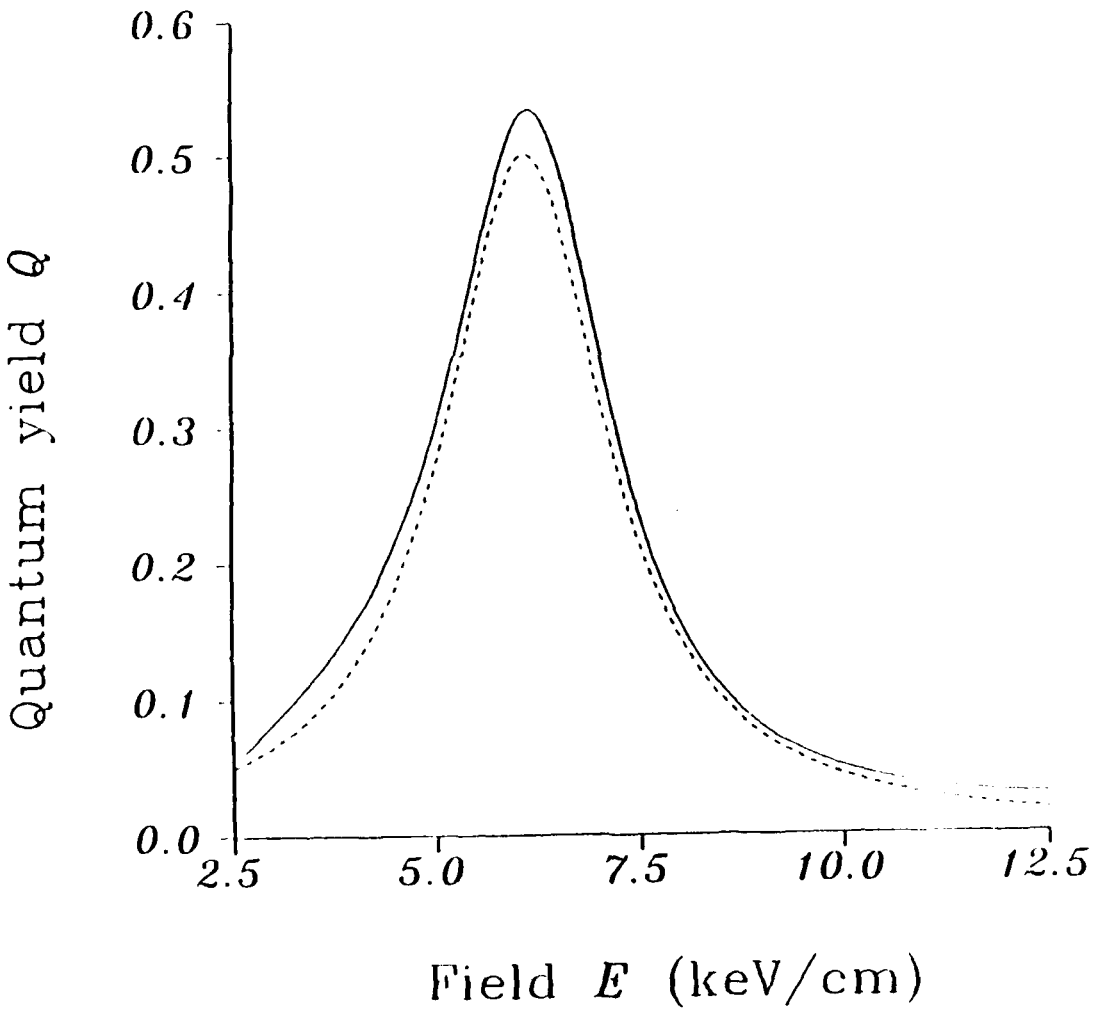

Mark I Stockman et all "Kinetics of intersubband..."

Fig. 3

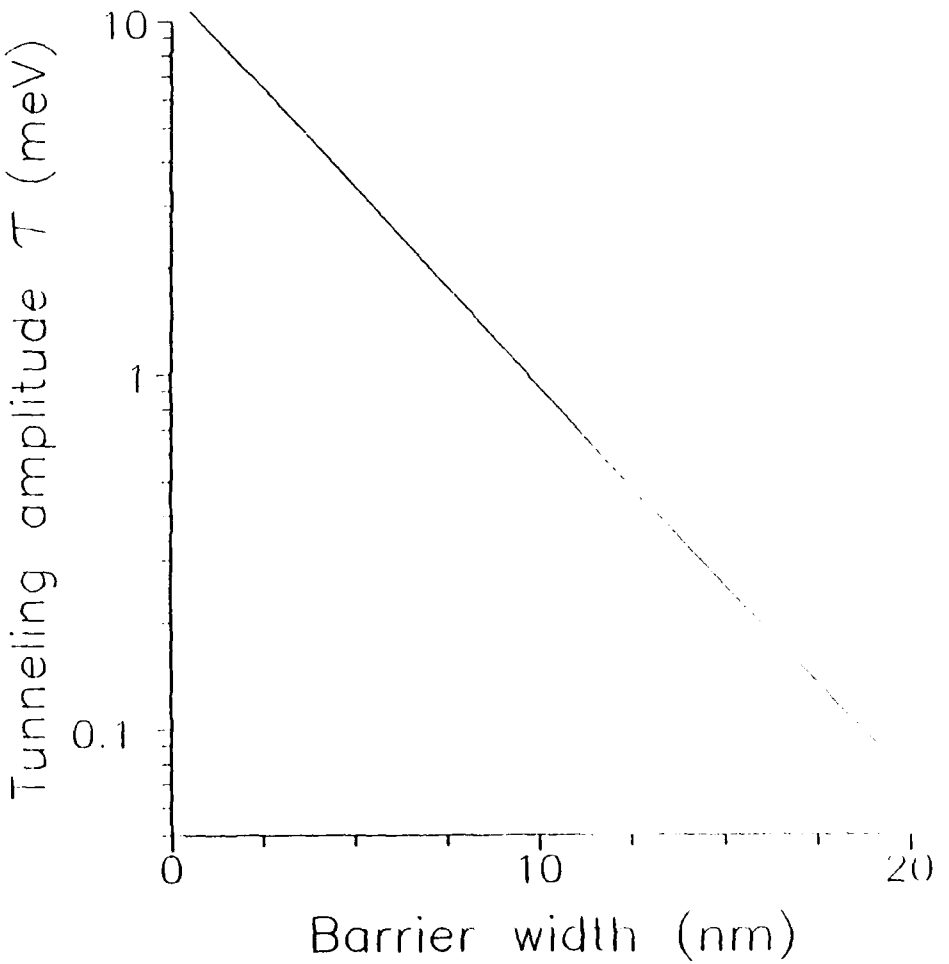

Marie C. Stockman et al

"Kinetics of intersubband..."

Fig. 4

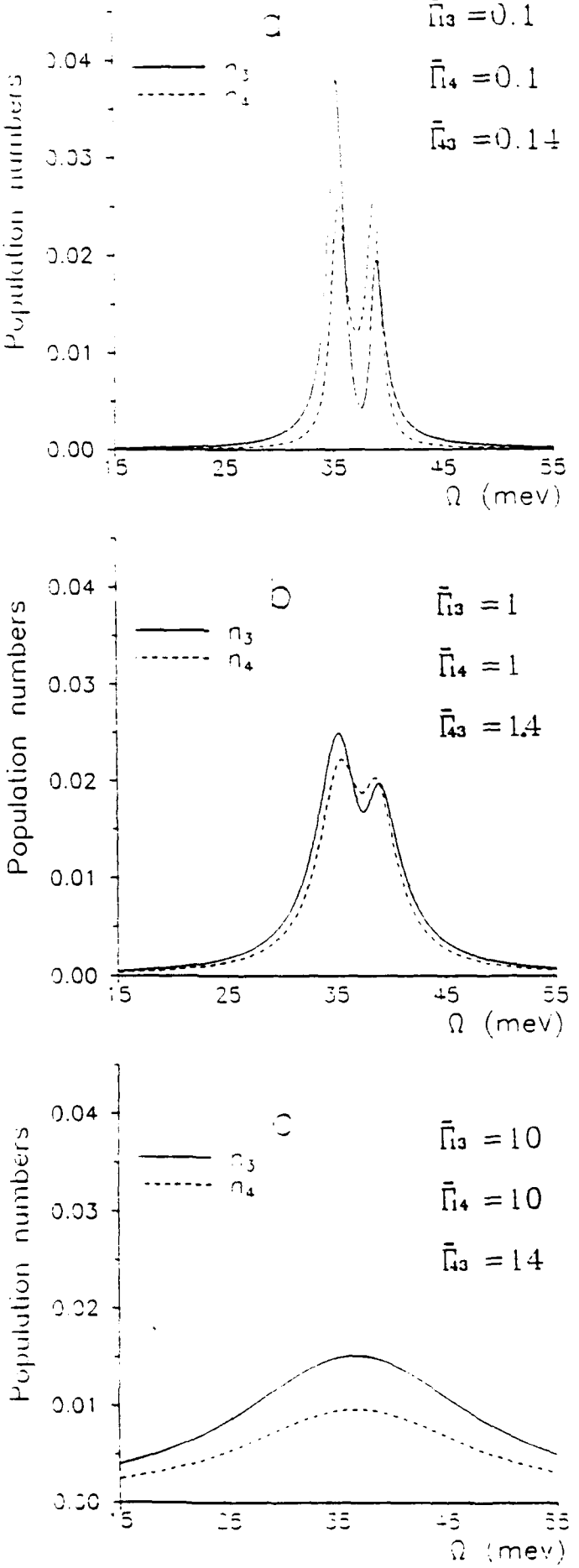

Mark I. Stockman
et all.
"Kinetics of inter-
subband..."

Fig. 5

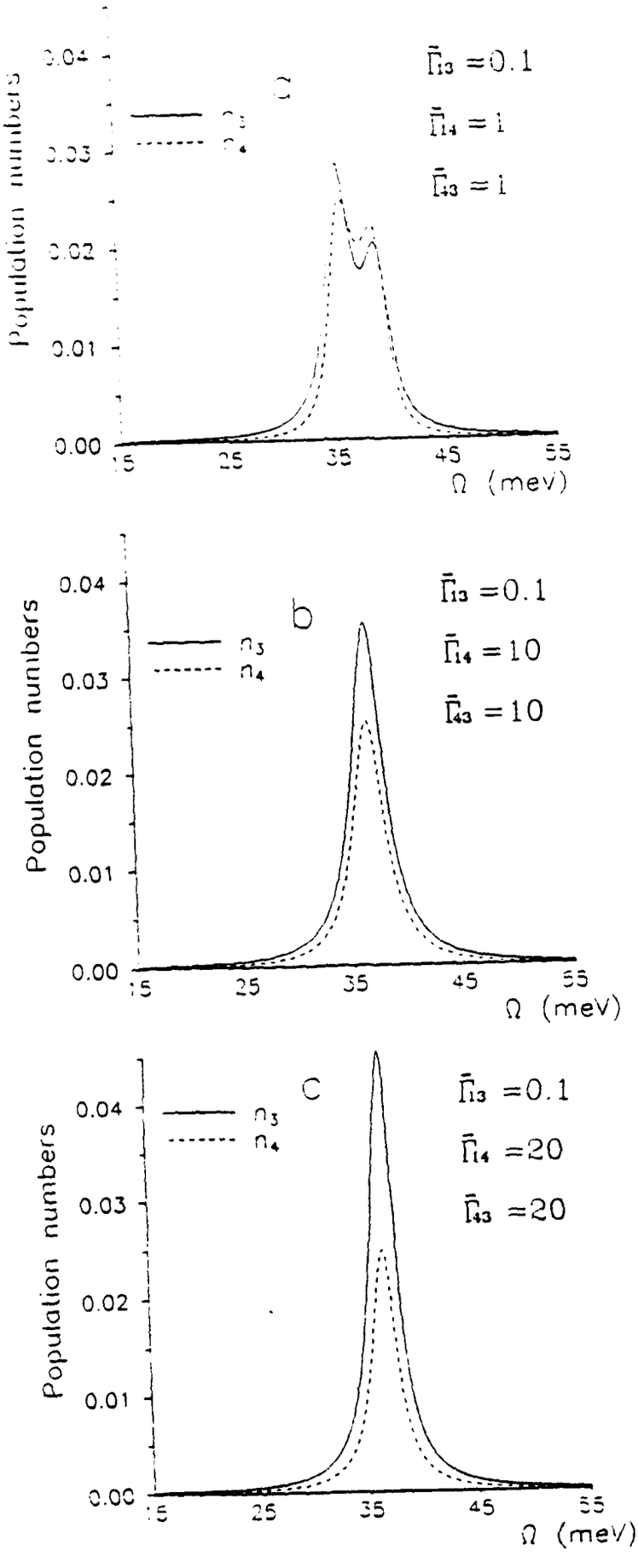

Mark I. Stockman
et all.

"Kinetics of
intersubband..."

Fig. 6